International Tables for Crystallography (2006). Vol. F, Section 7.2.2, pp. 148–149.

7.2. CCD detectors

BY M. W. TATE, E. F. EIKENBERRY AND S. M. GRUNER

7.2.1. Overview

After more than 20 years of refinement, CCD (charge-coupled device) detectors have emerged as the most useable and accurate large-area detectors available for the X-ray energies of interest to crystallographers. CCDs are familiar as the imagers in television and digital cameras, but the scientific grade devices used in detectors are larger and have more pixels and a lower noise amplifier. CCD detectors are an assembly of several components: an energy converter (*e.g.* phosphor), an optical relay with or without gain (fibre optics, lenses and/or intensifier) and the imaging CCD.

Although many configurations have been used in the past, improvements in the size and quality of fibre-optic tapers have led to the possibility of direct coupling – eliminating intensifiers and lenses – so long as other components are carefully optimized at the same time (Eikenberry *et al.*, 1991). Optimizations include the phosphor, the CCD and electronics, and the elimination of unneeded optical interfaces. Current commercial designs employ just three elements: phosphor, taper and CCD (Fig. 7.2.1.1). This concept enabled the use of large tapers, machined square at the front, that can be stacked together to form mosaic arrays. Consequently, there is now no inherent limit to the size of a CCD detector.

7.2.2. CCD detector assembly

Any practical detector requires compromises in the choice of components to optimize those aspects most important to the diffraction problem at hand. The optimization of one detector characteristic often adversely affects other characteristics, so that it is often difficult to identify the 'best' component. Considerations are given below to aid in making judicious choices.

Most fundamentally, a viable X-ray detector must have good quantum efficiency (see Section 7.1.1 in Chapter 7.1). Necessary, but not sufficient, are a high stopping power for X-rays and a large average signal per X-ray recorded in the CCD. The input signal passes through a sequence of stages and is transformed several times in the process. The statistics of this process are governed by the quantized nature of the signal, whether it be the initial X-ray photon, the visible photons produced in the phosphor, intermediate photoelectrons in intensifiers or the integrated charge in the CCD. To maintain a high detective quantum efficiency (DQE), the associated number of quanta per X-ray must be kept well above unity at each stage in the 'quantum chain'. There are several approaches that meet this criterion.

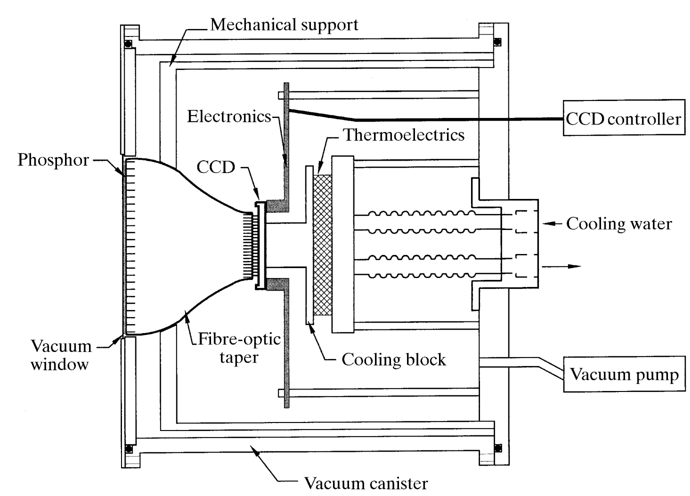

Fig. 7.2.1.1. Schematic of a single-module CCD detector. The thin phosphor screen is behind a light- and vacuum-tight vacuum window and is coupled to a fibre-optic taper, which is, in turn, coupled to a CCD. The CCD is thermoelectrically cooled to 213 K and housed in a vacuum cryostat. Reproduced with permission from Tate *et al.* (1995). Copyright (1995) International Union of Crystallography.

Crystallography applications generally benefit from large detective areas, whereas typical scientific CCDs are quite modest in size (*circa* 25×25 mm). The usual solution is to use fibre-optic tapers (which are more efficient demagnifiers than lenses; see Deckman & Gruner, 1986) to optically reduce a diffraction image excited in a larger phosphor screen. However, since optical image reduction is inherently inefficient, the reduction ratio is usually limited to about 4:1 before the number of visible photons per X-ray transmitted to the CCD becomes unacceptably low. Higher reduction ratios require image intensification *before* reduction (Moy, 1994; Naday *et al.*, 1995; Tate *et al.*, 1997) or there will be an unacceptable loss in DQE. Intensification *after* reduction can result in the same average recorded signal per X-ray. However, there is a significant probability that no quanta at all make it through the chain for many of the incident X-rays, thereby lowering the number of X-rays actually 'counted'.

Properties of the individual components affect other important detector characteristics as well. Below is a summary of important parameters for each of the components. Performance variations of CCD detectors from different vendors can most often be traced to the quality of the phosphor screen and the calibrations that are applied to the detector.

Phosphors. Although there are a bewildering variety of phosphor types, only a few are typically used with X-ray detectors (Shepherd *et al.*, 1995). A dense, high atomic number material is necessary to make the thin screens required for good spatial resolution while maintaining high X-ray stopping power. Gd_2O_2S:Eu offers high light output (> 200 visible photons per 8 keV X-ray) and an emission spectrum matched to the typical CCD's spectral sensitivity peak in the red. Although there is a fairly prompt emission of most of the light (< 1 ms to 10%), there is a long-term persistence which decays according to a power law: bright spots glow for seconds after an exposure has ended. This severely limits the dynamic range during fast framing, such as might be encountered in a synchrotron environment.

Other dopants for Gd_2O_2S, such as Tb and Pr, have much shorter persistence and are better suited to higher frame rates. These phosphors yield somewhat lower CCD signals because they emit fewer visible photons per X-ray and because their blue–green emission is less well matched to the CCD spectral sensitivity. Interestingly, Gd_2O_2S:Tb has one of the slowest 'prompt' emission (exponential decay) time constants, but is one of the fastest phosphors to decay to 10^{-4} (< 10 ms), resulting in low persistence.

Thicker phosphors are needed at higher X-ray energies (>15 keV) to maintain high stopping power. This generally reduces spatial resolution. However, structured phosphors offer a way to increase thickness while limiting the lateral spread of the light. For example, CsI:Tl can be grown as an array of columnar crystals, resulting in a screen with enhanced resolution (Stevels & Schrama-de Pauw, 1974*a*,*b*; Moy, 1998). The spectral mismatch of this green-emitting phosphor is offset by the increased signal per X-ray expected at these higher X-ray energies. Recently, a (Zn,Cd)Se phosphor has been described that has excellent characteristics for X-ray energies above 12 keV; the stopping power at lower energies is compromised by absorption edges (Bruker AXS Inc.).

Fibre optics and lenses. Light transmission in image reduction is limited by n.a. $\times M^2$, where n.a. is the numerical aperture of the optical system and M is the linear magnification factor ($M < 1$ corresponds to reduction). Lens systems have low values of n.a. when used in reduction, so there is only 2% light transmission for a 3:1 reduction with an f/1.0 lens. With a much higher n.a., fibre optics can typically transmit 13% with the same 3:1 reduction (Coleman, 1985). Such reducing tapers are produced by locally heating, then pulling, a fused bundle of optical fibres. Each fibre within the bundle becomes tapered in this process, thereby reducing the image scale from front to back of the bundle. The bundle structure introduces a characteristic 'chicken-wire' pattern into the image which must be removed *via* intensity calibration (Section 7.2.3). Tapers up to 165 mm in diameter are available.

To obtain good resolution, extramural absorbing fibres (EMAs) must be placed in the fibre optic to absorb light that propagates between fibres. These EMAs are often a more effective absorber in the blue part of the spectrum, with the result that a red-emitting phosphor yields somewhat poorer resolution. Another concern with fibre optics is radioactivity in the glass used to produce the optic, which manifests itself as random flashes ('zingers') in both the phosphor and the CCD (Section 7.2.3).

Although fibre-optic coupling is preferred in many situations, lenses are appropriate for use with image intensification, or in cases of image magnification, such as for microtomography, using high-resolution screens.

Image intensifiers allow large demagnification ratios without undue DQE loss (Moy, 1994). In these vacuum-tube devices, visible light produces photoelectrons in the photocathode of the intensifier, which in turn are accelerated under high potential onto a secondary phosphor screen. Each photoelectron excites many photons in the secondary phosphor, giving light amplification. Image resolution is retained either by magnetic, electrostatic or proximity focusing of the electrons. In the case of microchannel plate intensifiers, photoelectrons are restricted to cascade down hollow fibres. Intensifiers often have problems with stability and linearity, and they degrade resolution. Phosphor afterglow in the secondary phosphors is also a consideration. Intensifiers typically limit the input format to less than 80 mm in diameter, although one design uses a large (230 mm) radiographic intensifier (Moy, 1994; Hammersley *et al.*, 1997). The greatest drawbacks of image intensifiers are cost, availability, susceptibility to magnetic fields and lack of robustness.

CCDs. The low noise and high sensitivity of scientific CCDs have made CCDs the preferred imaging device in X-ray applications. Visible photons are converted to charge carriers in the silicon of the CCD, with a 30–40% quantum efficiency (q.e.) in the red, dropping to 5% in the blue owing to increased absorption by the controlling gate structure (the q.e. can be considerably higher for back-illuminated devices which, however, are expensive, fragile and difficult to obtain). The 'read noise' (noise with zero charge in the pixel) is routinely less than 10 electrons for scientific grade chips with pixel read rates of less than 1 MHz. When coupled to a good phosphor screen with a modest (*circa* 3:1) fibre-optic taper, signal levels in the CCD are typically 10–30 recorded electrons per 10 keV X-ray. This is above the CCD read-noise level, thereby allowing low-dose quantum-limited X-ray imaging.

A physically large CCD chip is usually desired to maximize the detector area, given the limited image reduction ratio. Devices from 2–4 cm on an edge with 1000×1000 to 2000×2000 pixels are available. These sizes match well to the largest of the fibre-optic tapers and are therefore most often used in detectors. Larger-format CCDs are available, but are harder to obtain and are expensive.

CCDs are usually cooled well below room temperature to minimize thermally generated dark current, an unwanted source of noise. The dark current drops by a factor of 2 for every 5–7 K drop in temperature. At 233 K, there is roughly one electron per pixel per second dark current for normal clocking operation. Since the dark current changes with temperature, the temperature must be well regulated (to within ± 0.1 K) to subtract the dark charge from an image reproducibly.

Most of the dark current comes from surface defects, not from the bulk silicon. Multiphase pinned (MPP) CCDs use charge implants within the pixel structure to move the charge collection region away from the surface, thereby reducing the dark current by several orders of magnitude. This is usually accompanied by a significant reduction in the maximum charge capacity ('full well') of a pixel. Even so, MPP CCDs are becoming the norm in most X-ray detectors.

Directly exposed CCDs. CCDs can directly image X-rays, although typical CCDs are not very efficient, since the charge collection region in the silicon is very thin (< 10 μm). Thicker depletion regions can be fabricated in high-resistivity silicon wafers, improving X-ray collection efficiency to greater than 30% at 8 keV. Direct conversion of X-rays in silicon produces a large signal with excellent energy resolution. It is therefore possible to use the chip as an X-ray counting detector with the ability to discriminate in energy. To retain X-ray-energy measurement capability, however, there must be less than one X-ray per pixel per frame to avoid signal overlap. This requires a fast readout as well as large amounts of disk storage to handle the large number of files. The X-rays damage the CCD's electronic structure, resulting in a higher dark current within the exposed pixels. Care must be taken to shield non-imaging parts of the CCD, such as the output amplifier, which will adversely affect chip performance at even lower radiation dose.

7.2.3. Calibration and correction

Inhomogeneities within the detector components introduce non-uniformities in the output image of several per cent or more, both as geometric distortion and as nonuniformity of response. The response of the system varies not only with position, but also with the angle of incidence and X-ray energy. Optimal calibration of the detector should take into account the parameters of the X-ray experiment, seeking to mimic the experimental conditions as closely as possible: a uniform source of X-rays of the proper energy positioned in place of the diffracting crystal would be ideal. Realizing such a source is somewhat problematic, so the calibration procedure is often broken down into several independent steps. Calibration procedures are detailed in Barna *et al.* (1999) and are summarized below.

7.2.3.1. *Dark-current subtraction*

It is important to remove both the electronic offset and the accumulated dark charge from an X-ray image. Since the integrated dark current varies from pixel to pixel and with time, a set of images needs to be taken (with no X-rays), matched in integration time to the X-ray exposures. With a properly temperature-stabilized detector, the background images may be acquired in advance and used throughout an experiment. Because the background image has noise, it is common to average a number of separate backgrounds to minimize the noise.

7.2.3.2. *Removal of radioactive decay events*

Cosmic rays and radioactive decay of actinides in the fibre-optic glass produce large-amplitude isolated signals ('zingers') within an X-ray image. These accumulate randomly in position and in time. For the short exposures typical at synchrotron sources and for data sets with highly redundant information, the few diffraction spots

references